

RUNNING CRACK IN AN INCIDENT WAVE FIELD

E. P. CHEN and G. C. SIH

Institute of Fracture and Solid Mechanics, Lehigh University, Bethlehem, Pennsylvania 18015

Abstract—Steady-state diffraction of stress waves by a semi-infinite running crack is considered in this study. In conjunction with the principle of superposition, an exact solution is obtained by using a method based on the Wiener-Hopf technique. As in the static case, the dynamic stresses possess the familiar inverse square-root singularity at the crack tip. The stress-intensity factors, however, are found to depend on the incident wave length, angle of incidence, Poisson's ratio of the elastic solid and speed of crack propagation. The stress-intensity factor serves as a useful parameter in studying elasto-dynamic crack problems since it can be associated with the rate at which elastic and kinetic energies are released by the crack. Ductile fracture is studied by adapting the Dugdale's hypothesis. The length of the plastic zone is determined and the influence of the speed of crack propagation is displayed graphically.

1. INTRODUCTION

UNDER dynamic loading, the action of external forces is transmitted to all parts of the structure in the form of stress waves. At the crack, the waves are refracted and reflected causing a high stress elevation near the crack tip. This may lead to gradual crack extension and perhaps result in the ultimate failure of the structure.

The scattering of waves by cracks of various geometries has been the subject of many past investigations. Ang and Knopoff [1, 2] have treated the problems of a finite crack subject to anti-plane shear, compression and in-plane shear waves. Their results, however, are valid only for low frequencies and large distances from the line of discontinuity. Using an integral transform technique, Sih and Loeber [3-6] were able to furnish near-field solutions to a class of diffraction problems with various crack configurations. Transient problems of a crack subject to impulsive loadings were considered by Baker [7], Ravera [8], Embley [9] and Thau and Lu [10, 11]. Baker treated the case of a semi-infinite crack propagating at constant velocity after it had appeared suddenly in the stretched elastic body. Ravera, Thau and Lu considered the problem of a double-ended crack subject to in-plane and anti-plane impact loadings. The axisymmetric problem of a penny-shaped crack influenced by step loadings was solved by Embley. Based on a method by Evvard [12] and Kostrov [13], Achenbach [14-17] solved a class of transient elasto-dynamic crack problems. The salient feature of his work is the presentation of the rate of energy balance in the fracture process.

Another type of elasto-dynamic crack problem has also received much attention. This is the type of problem of a crack propagating under the influence of uniform loading conditions. Yoffe [18] studied the case of a constant length crack propagating through an

infinite elastic medium. The corresponding semi-infinite crack problem was treated by Craggs [19]. The more realistic problem of a crack whose tips are expanding in opposite directions was solved by Broberg [20] and Craggs [21]. The axisymmetric problem of an expanding penny-shaped crack was considered by Atkinson [22] and Kostrov [23].

Although much has been done in the foregoing problem areas, an understanding of crack propagation induced by dynamic loading conditions has not yet been achieved. Certain information has been given by Janhanshahi [24], who solved the problem of diffraction of horizontally polarized shear waves by a semi-infinite crack extending uniformly under the condition of anti-plane strain. The same problem with a finite length crack has been studied by Sih and Loeber [25]. These problems correspond to Mode III problems in the static theory of fracture. The corresponding in-plane problems are considered to be more significant since most structural members are subjected to oscillating loads undergoing tension-compression cycles. However, the analysis is considerably more difficult since both plane compressional and vertically polarized shear waves are developed after either type of incident wave is scattered from the crack. In addition, Raleigh surface waves are generated along the crack surfaces. Mathematically, instead of one wave equation to be solved for Mode III problem, two wave equations must be considered for the in-plane problems.

In this paper the interaction of stress waves with a semi-infinite running crack under either the plane strain or the generalized plane stress condition is considered. Employing the principle of superposition and a method based on the Wiener-Hopf technique, an attempt is made to obtain an exact solution to the stated problem. The dynamic stress-intensity factor, the energy release rate and the crack surface displacement will be expressed in terms of crack speed, angle of incidence and Poisson's ratio of the elastic solid and will be displayed graphically to show the effect of these parameters.

Ductile fracture is included in the present study by the application of Dugdale's hypothesis [26] which has subsequently been extended to dynamic problems by Goodier and Fields [27], Atkinson [28], Kanninen [29] and Embley and Sih [30]. The attractive feature of this model is simplicity, and although it does not provide a satisfactory approximation to the stress distribution, it appears to be useful in determining such gross characteristics as the length of the plastic zone. Other flow characteristics of the material such as strain hardening, strain rate, etc., may also be included in the Dugdale model. A study of this kind has recently been carried out by Kanninen, Mukherjee *et al.* [31] who investigated the influence of the dynamic flow properties of metals on the speed of ductile crack propagation.

2. FORMULATION OF THE PROBLEM

Field equation and input waves

Consider the propagation of elastic waves which vary harmonically in time and are applied in the XY -plane containing a through crack which is semi-infinite in length and is extending along $Y = 0$ at a constant rate v . Both compressional (P-) and shear (SV-) waves arise in the plane and the resulting displacement and stress fields can be expressed in terms of two scalar functions Φ_1 and Φ_2 each of which depends on X , Y and t . The

rectangular components of the displacement and stress fields are:

$$\begin{aligned}
 (U_X, V_Y, W_Z) &= \left(\frac{\partial \Phi_1}{\partial X} + \frac{\partial \Phi_2}{\partial Y}, \frac{\partial \Phi_1}{\partial Y} - \frac{\partial \Phi_2}{\partial X}, 0 \right), \\
 \sigma_X &= \lambda \nabla^2 \Phi_1 + 2\mu \left(\frac{\partial^2 \Phi_1}{\partial X^2} + \frac{\partial^2 \Phi_2}{\partial X \partial Y} \right), \\
 \sigma_Y &= \lambda \nabla^2 \Phi_1 + 2\mu \left(\frac{\partial^2 \Phi_1}{\partial Y^2} - \frac{\partial^2 \Phi_2}{\partial X \partial Y} \right), \\
 \sigma_{XY} &= \mu \left(2 \frac{\partial^2 \Phi_1}{\partial X \partial Y} - \frac{\partial^2 \Phi_2}{\partial X^2} + \frac{\partial^2 \Phi_2}{\partial Y^2} \right)
 \end{aligned} \tag{2.1}$$

in which λ is the Lamé constant and μ stands for the shear modulus of elasticity.

Substituting equation (2.1) into the equation of motion of an isotropic elastic solid, the following wave equations on Φ_1 and Φ_2 are obtained:

$$\nabla^2 \Phi_k - \frac{1}{C_k^2} \frac{\partial^2 \Phi_k}{\partial t^2} = 0, \quad k = 1, 2. \tag{2.2}$$

In equation (2.2), C_1 and C_2 are respectively the velocities of compressional and shear waves in an infinitely extended elastic medium and they are given by

$$\begin{aligned}
 C_1^2 &= \frac{\lambda + 2\mu}{\rho}, & C_2^2 &= \frac{\mu}{\rho}, \\
 C^2 = C_2^2/C_1^2 &= \begin{cases} (1-2\nu)/2(1-\nu), & \text{plane strain} \\ (1-\nu)/2, & \text{generalized plane stress} \end{cases}
 \end{aligned} \tag{2.3}$$

where ρ is the mass density and ν is the Poisson's ratio.

Define two moving coordinate systems by

$$t = t, \quad x_k = X - vt, \quad y_k = S_k Y, \quad k = 1, 2 \tag{2.4}$$

where

$$S_k = \sqrt{1 - M_k^2} \quad \text{and} \quad M_k = v/C_k. \tag{2.5}$$

In equation (2.5), M_1 and M_2 are known as the Mach numbers. With respect to the moving systems, equation (2.2) becomes

$$\frac{\partial^2 \Phi_k}{\partial x_k^2} + \frac{\partial^2 \Phi_k}{\partial y_k^2} + \frac{2M_k}{C_k S_k^2} \frac{\partial^2 \Phi_k}{\partial x_k \partial t} - \frac{1}{C_k^2 S_k^2} \frac{\partial^2 \Phi_k}{\partial t^2} = 0, \quad k = 1, 2 \tag{2.6}$$

in which Φ_k is now a function of x_k , y_k and t . Input waves from infinity in the fixed coordinate system may be written as

$$\Phi_k^{(i)} = \Phi_k \exp\{-i\Lambda_k [X \cos \Theta_k + Y \sin \Theta_k] - i\Omega t\}, \quad k = 1 \quad \text{or} \quad 2, \tag{2.7}$$

in which

$$\begin{aligned} \Omega &= \text{circular frequency,} \\ \Lambda_k &= \frac{\Omega}{C_k} = \text{wave number,} \\ \Theta_k &= \text{angle of incidence,} \\ \phi_k &= \text{wave amplitude.} \end{aligned} \tag{2.8}$$

In the moving systems, equation (2.7) takes the form

$$\Phi_k^{(i)} = \phi_{kk}^{(i)}(x_k, y_k) \exp\{iM_k \lambda_{kk} x_k - i\omega_k t\} \tag{2.9}$$

where

$$\begin{aligned} \phi_{kk}^{(j)} &= \phi_k \exp\{-i\lambda_{kk}[x_k \cos \theta_k + y_k \sin \theta_k]\}, \\ \cos \theta_k &= \frac{M_k + \cos \Theta_k}{\alpha_k}, \quad \sin \theta_k = \frac{S_k}{\alpha_k} \sin \Theta_k, \\ \alpha_k &= 1 + M_k \cos \Theta_k, \quad \lambda_{kk} = \frac{\Lambda_k}{S_k^2} \alpha_k = \text{apparent wave number} \\ &\omega_k = \alpha_k \Omega. \end{aligned} \tag{2.10}$$

Guided by the above as well as by the objective of eliminating the mixed derivative term in equation (2.6), assume the solution to the governing equations as

$$\Phi_{jk} = \phi_{jk}(x_k, y_k) \exp\{iM_k \lambda_{jk} x_k - i\omega_j t\} \tag{2.11}$$

with

$$\lambda_{jk} = \frac{\Lambda_k}{S_k^2} \alpha_j, \quad j, k = 1, 2 \tag{2.12}$$

where $j = 1$ or 2 corresponds to the type of input wave and $k = 1$ or 2 corresponds to the two wave potentials. In the subsequent discussion it is to be understood that the subscripts j and k have the above meaning.

Substitution of equation (2.11) into equation (2.6) yields

$$\frac{\partial^2 \phi_{jk}}{\partial x_k^2} + \frac{\partial^2 \phi_{jk}}{\partial x_k^2} + \lambda_{jk}^2 \phi_{jk} = 0, \quad j, k = 1, 2 \tag{2.13}$$

which is the Hemholtz equation.

Scattered-wave potentials

The total wave field may be taken as the linear sum of the displacement potentials of the incident and scattered waves as

$$\Phi_k = \Phi_k^{(i)} + \Phi_k^{(s)}, \quad k = 1, 2. \tag{2.14}$$

Since the incident wave field is already a solution to the wave equation, the main analysis lies in the determination of the scattered-wave potentials $\Phi_k^{(s)}$, $k = 1, 2$. In view of equation (2.11) the scattered potential $\phi_{jk}^{(s)}$ in the moving coordinate system is governed by the Hemholtz equation

$$\frac{\partial^2 \phi_{jk}^{(s)}}{\partial x_k^2} + \frac{\partial^2 \phi_{jk}^{(s)}}{\partial y_k^2} + \lambda_{jk}^2 \phi_{jk}^{(s)} = 0, \quad j, k = 1, 2 \tag{2.15}$$

where

$$\phi_{jk}^{(s)} \rightarrow 0 \quad \text{as} \quad (x_k^2 + y_k^2)^{\frac{1}{2}} \rightarrow \infty.$$

The same general relationship applies to the total displacement and stress fields.

Equation (2.15) can be solved by applying a Fourier transform and the result is

$$\phi_{jk}^{(s)}(x_k, y_k) = \frac{1}{2\pi} \int_{-\infty}^{\infty} A_{jk}(\xi) \exp\{-i\xi x_k - \gamma'_{jk} y_k\} d\xi, \quad j, k = 1, 2, \quad y_k \geq 0 \quad (2.16)$$

in which $A_{jk}(\xi)$ is the unknown to be determined. The branch cut of the functions

$$\gamma'_{jk} = (\xi^2 - \lambda_{jk}^2)^{\frac{1}{2}} = -i(\lambda_{jk}^2 - \xi^2)^{\frac{1}{2}} \quad (2.17)$$

has already been discussed by Noble [32]; therefore, no additional comment will be made here.

At this point, it is convenient to define

$$\begin{bmatrix} U_X \\ V_Y \\ \sigma_X \\ \sigma_Y \\ \sigma_{XY} \end{bmatrix} = \begin{bmatrix} u_x \\ v_y \\ \sigma_x \\ \sigma_y \\ \sigma_{xy} \end{bmatrix} \exp\{iM_j \lambda_{jj} x_s - i\omega_j t\} \quad (2.18)$$

such that in dealing with $(u_x, v_y, \sigma_x, \sigma_y, \sigma_{xy})$ the same exponential factor is suppressed.

Using the derivatives of ϕ_k and the notation

$$\beta_{jk} = M_j \lambda_{jj} \left(1 - \frac{\lambda_{jk} C_j}{\lambda_{jj} C_k} \right), \quad j, k = 1, 2 \quad (2.19)$$

the expressions for the displacements and stresses become

$$\begin{aligned} u_x^{(s)} &= \frac{1}{2\pi} \int_{-\infty}^{\infty} \{-i(\xi - M_j \lambda_{jj}) A_{j1}(\xi) \exp(-\gamma_{j1} y_1) - S_2 \gamma_{j2} A_{j2}(\xi) \exp(-\gamma_{j2} y_2)\} \exp(-i\xi x) d\xi, \\ v_y^{(s)} &= \frac{1}{2\pi} \int_{-\infty}^{\infty} \{-S_1 \gamma_{j1} A_{j1}(\xi) \exp(-\gamma_{j1} y_1) + i(\xi - M_j \lambda_{jj}) A_{j2}(\xi) \exp(-\gamma_{j2} y_2)\} \exp(-i\xi x) d\xi, \\ \frac{\sigma_x^{(s)}}{2\mu} &= \frac{1}{2\pi} \int_{-\infty}^{\infty} \left\{ \left[-\frac{1}{2C^2} (\xi - M_j \lambda_{jj})^2 + \left(\frac{1}{2C^2} - 1 \right) S_1^2 \gamma_{j1}^2 \right] \right. \\ &\quad \left. \times A_{j1}(\xi) \exp(-\gamma_{j1} y_1) + i S_2 \gamma_{j2} (\xi - M_j \lambda_{jj}) A_{j2}(\xi) \exp(-\gamma_{j2} y_2) \right\} \exp(-i\xi x) d\xi, \\ \frac{\sigma_y^{(s)}}{2\mu} &= \frac{1}{2\pi} \int_{-\infty}^{\infty} \left\{ \left[-\left(\frac{1}{2C^2} - 1 \right) (\xi - M_j \lambda_{jj})^2 + \frac{S_1^2}{2C^2} \gamma_{j1}^2 \right] \right. \\ &\quad \left. \times A_{j1}(\xi) \exp(-\gamma_{j1} y_1) - i S_2 \gamma_{j2} (\xi - M_j \lambda_{jj}) A_{j2}(\xi) \exp(-\gamma_{j2} y_2) \right\} \exp(-i\xi x) d\xi, \\ \frac{\sigma_{xy}^{(s)}}{2\mu} &= \frac{1}{2\pi} \int_{-\infty}^{\infty} \{ i S_1 \gamma_{j1} (\xi - M_j \lambda_{jj}) A_{j1}(\xi) \exp(-\gamma_{j1} y_1) + \frac{1}{2} [S_2^2 \gamma_{j2}^2 + (\xi - M_j \lambda_{jj})^2] A_{j2}(\xi) \\ &\quad \times \exp(-\gamma_{j2} y_2) \} \exp(-i\xi x) d\xi, \quad j = 1, 2 \end{aligned} \quad (2.20)$$

where

$$\gamma_{jk} = [(\xi - \beta_{jk})^2 - \lambda_{jk}^2]^{\frac{1}{2}}. \tag{2.21}$$

Note that in deriving equations (2.20) the relation $x_1 = x_2 = x$ has been used.

Boundary conditions

For a traction-free crack surface, the total normal and shear stresses must vanish on L , the region the crack occupies, i.e.,

$$\begin{aligned} \sigma_y^{(i)}(x, 0) + \sigma_y^{(s)}(x, 0) &= 0, & x \in L \\ \sigma_{xy}^{(i)}(x, 0) + \sigma_{xy}^{(s)}(x, 0) &= 0, & x \in L \end{aligned} \tag{2.22}$$

from which the boundary conditions of the scattered-wave problems may be established. For convenience, the problem will be split into two parts, namely, that of finding the solution of equation (2.15) for the following conditions:

Case A.

$$\begin{aligned} v_x^{(s)}(x, 0) = \sigma_{xy}^{(s)}(x, 0) &= 0, & x \notin L \\ \sigma_y^{(s)}(x, 0) = -\sigma_y^{(i)}(x, 0); & \quad \sigma_{xy}^{(s)}(x, 0) = 0, & x \in L \end{aligned} \tag{2.23}$$

Case B.

$$\begin{aligned} u_x^{(s)}(x, 0) = \sigma_y^{(s)}(x, 0) &= 0, & x \notin L \\ \sigma_y^{(s)}(x, 0) = 0; & \quad \sigma_{xy}^{(s)} = -\sigma_{xy}^{(i)}(x, 0), & x \in L. \end{aligned} \tag{2.24}$$

It is evident that the stress solutions for Case A and Case B are even and odd in y , respectively; consequently, the former case will be called the symmetric problem and the latter the skew-symmetric problem. The complete solution to the original problem can be obtained by superposition of the solutions for the two cases.

Case A. Symmetric problem. The normal traction corresponding to the incident wave fields can be written as:

$$\frac{\sigma_y^{(i)}(x, 0)}{2\mu} = P_j \exp(-i\lambda_{jj}x \cos \theta_j), \quad j = 1, 2 \tag{2.25}$$

where

$$P_1 = \lambda_{11}^2 \left\{ -\left(\frac{1}{2C^2} - 1 \right) (M_1 - \cos \theta_1)^2 - \left(\frac{S_1^2}{2C^2} \right) \sin^2 \theta_1 \right\} \phi_1 \tag{2.26}$$

corresponds to the incident P-wave, and

$$P_2 = -S_2^2 \lambda_{22}^2 \sin \theta_2 (M_2 - \cos \theta_2) \phi_2 \tag{2.27}$$

to the incident SV-wave. Define a function $A_j(\xi)$ through

$$\left\{ \begin{aligned} A_{j1}(\xi) \\ A_{j2}(\xi) \end{aligned} \right\} = \frac{2A_j(\xi)}{[(\xi - M_j \lambda_{jj})^2 - S_2^2 \gamma_{j2}^2]} \left\{ \begin{aligned} + \frac{[S_2^2 \gamma_{j2}^2 + (\xi - M_j \lambda_{jj})^2]}{2S_1 \gamma_{j1}} \\ - i(\xi - M_j \lambda_{jj}) \end{aligned} \right\}. \tag{2.28}$$

Making use of equations (2.20), (2.28) and boundary conditions (2.23), a set of dual integral equations is obtained :

$$\begin{aligned} \frac{1}{2\pi} \int_{-\infty}^{\infty} A_j(\xi) \exp(-i\xi x) d\xi &= 0, \quad x \notin L \\ \frac{1}{2\pi} \int_{-\infty}^{\infty} f_j(\xi) A_j(\xi) \exp(-i\xi x) d\xi &= -P_j \exp(-i\lambda_{jj}x \cos \theta_j), \quad x \in L \end{aligned} \tag{2.29}$$

where

$$\begin{aligned} f_j(\xi) = \left\{ - \left[\left(\frac{1}{2C^2} - 1 \right) (\xi - M_j \lambda_{jj})^2 - \frac{S_1^2}{2C^2} \gamma_{j1}^2 \right] [(\xi - M_j \lambda_{jj})^2 + S_2^2 \gamma_{j2}^2] \right. \\ \left. - 2S_1 S_2 \gamma_{j1} \gamma_{j2} (\xi - M_j \lambda_{jj})^2 \right\} / S_1 \gamma_{j1} [(\xi - M_j \lambda_{jj})^2 - S_2^2 \gamma_{j2}^2]. \end{aligned} \tag{2.30}$$

Case B. Skew-symmetric problem. The shearing stress corresponding to the incident wave fields are

$$\frac{\sigma_{xy}^{(j)}(x, 0)}{2\mu} = Q_j \exp(-i\lambda_{jj}x \cos \theta_j), \quad j = 1, 2 \tag{2.31}$$

where

$$Q_1 = S_1 \lambda_{11}^2 \sin \theta_1 (M_1 - \cos \theta_1) \phi_1 \tag{2.32}$$

corresponds to the P-wave incidence, and

$$Q_2 = \frac{1}{2} \lambda_{22}^2 [(M_2 - \cos \theta_2)^2 - S_2^2 \sin^2 \theta_2] \phi_2 \tag{2.33}$$

to the SV-wave incidence.

Making use of equations (2.20) and (2.31) and replacing the unknowns A_{jk} by C_{jk} , $j, k = 1, 2$, boundary conditions (2.24) render

$$\begin{aligned} \frac{1}{2\pi} \int_{-\infty}^{\infty} C_j(\xi) \exp(-i\xi x) d\xi &= 0, \quad x \notin L \\ \frac{1}{2\pi} \int_{-\infty}^{\infty} q_j(\xi) C_j(\xi) \exp(-i\xi x) d\xi &= -Q_j \exp(-i\lambda_{jj}x \cos \theta_j), \quad x \in L \end{aligned} \tag{2.34}$$

in which

$$\begin{aligned} q_j(\xi) = \left\{ -C^2 \left[\left(\frac{1}{2C^2} - 1 \right) (\xi - M_j \lambda_{jj})^2 - \frac{S_1^2}{2C^2} \gamma_{j1}^2 \right] \right. \\ \left. \times [(\xi - M_j \lambda_{jj})^2 + S_2^2 \gamma_{j2}^2] - 2S_1 S_2 \gamma_{j1} \gamma_{j2} (\xi - M_j \lambda_{jj})^2 \right\} / [(\xi - M_j \lambda_{jj})^2 - S_2^2 \gamma_{j2}^2] S_2 \gamma_{j2}. \end{aligned} \tag{2.35}$$

In equation (2.34) the new unknown $C_j(\xi)$ is defined by

$$\begin{Bmatrix} C_{j1}(\xi) \\ C_{j2}(\xi) \end{Bmatrix} = \frac{2C^2 C_j(\xi)}{[(\xi - M_j \lambda_{jj})^2 - S_1^2 \gamma_{j1}^2]} \begin{Bmatrix} i(\xi - M_j \lambda_{jj}) \\ \frac{(1/2C^2)[(\xi - M_j \lambda_{jj})^2 - S_1^2 \gamma_{j1}^2] + (\xi - M_j \lambda_{jj})^2}{S_2 \gamma_{j2}} \end{Bmatrix}. \tag{2.36}$$

The objective in mind is to solve the pair of dual integral equations in equations (2.29) and (2.34) for the unknowns $A_f(\xi)$ and $C_f(\xi)$, respectively. Once this is done, all the stresses and displacements can be calculated through equations (2.28), (2.36) and (2.20).

3. SEMI-INFINITE CRACK PROBLEM

Solution to dual integral equations

Following the formulation in the last section, the problem will be separated into symmetric and skew-symmetric parts and each will be discussed individually. The geometry of the problem is shown in Fig. 1.

Case A. Symmetric problem. For this case, equations (2.29) have the form

$$\begin{aligned} \frac{1}{2\pi} \int_{-\infty}^{\infty} A_f(\xi) \exp(-i\xi x) d\xi &= 0, & x > 0 \\ \frac{1}{2\pi} \int_{-\infty}^{\infty} f_f(\xi) A_f(\xi) \exp(-i\xi x) d\xi &= -P_j \exp(-i\lambda_{jj}x \cos \theta_j), & x < 0. \end{aligned} \tag{3.1}$$

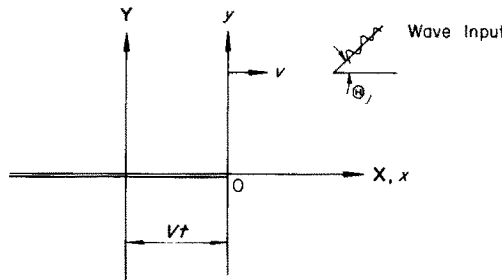


FIG. 1. Geometry of the semi-infinite running crack.

The solution to this set of dual integral equations may be obtained by a method based on the Wiener-Hopf technique. Define a new function $B_f(\xi)$ through

$$\begin{aligned} A_f(\xi) = S_1 \gamma_{j1} B_f(\xi) &= \{[(1 + M_1)(\xi - M_j \lambda_{jj}) - S_1^2 \lambda_{j1}] \\ &\times [(1 - M_1)(\xi - M_j \lambda_{jj}) + S_1^2 \lambda_{j1}]\}^{\frac{1}{2}} B_f(\xi). \end{aligned} \tag{3.2}$$

Making use of equation (3.2), equations (3.1) render

$$\begin{aligned} \frac{1}{2\pi} \int_{-\infty}^{\infty} S_1 \gamma_{j1} B_f(\xi) \exp(-i\xi x) d\xi &= 0, & x > 0 \\ \frac{1}{2\pi} \int_{-\infty}^{\infty} f'_f(\xi) B_f(\xi) \exp(-i\xi x) d\xi &= -P_j \exp(-i\lambda_{jj}x \cos \theta_j), & x < 0 \end{aligned} \tag{3.3}$$

where

$$f'_f(\xi) = S_1 \gamma_{j1} f_f(\xi). \tag{3.4}$$

The second of equations (3.3) is satisfied if

$$f'_j(\xi)B_j(\xi) = + \frac{K_{1j}}{2\pi i} \frac{U_{1j}(\xi)}{U_{1j}(\alpha_j)} \frac{1}{\xi - \alpha_j} \tag{3.5}$$

where

$$K_{1j} = -2\pi P_j, \quad \alpha_j = \lambda_{jj} \cos \theta_j. \tag{3.6}$$

In equation (3.5), $U_{1j}(\xi)$ is a function free from zeros and singularities in the upper ξ -plane except at infinity where it is required only to be of algebraic behavior. That equation (3.5) is a solution to the second of equations (3.3) is readily verified by completing the path from $-\infty$ to ∞ by a semi-circle of infinite radius in the upper ξ -plane, as shown in Fig. 2, and then applying the residue theorem and Jordan's Lemma. In Fig. 2, the path of integration is chosen to avoid the possible branch points and is indented below the pole

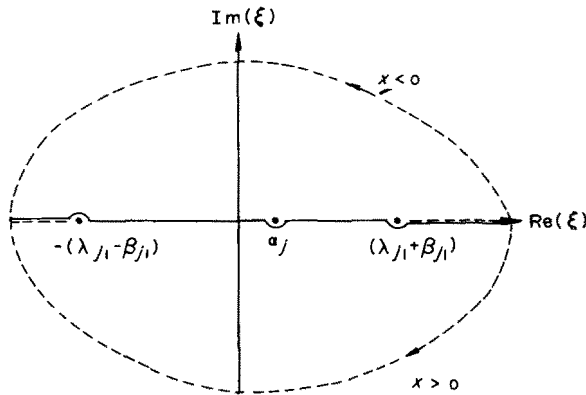


FIG. 2. The cut ξ -plane.

$\xi = \alpha_j$. Similarly, the first of equations (3.3) can be represented by

$$S_{1j}\gamma_{j1}B_j(\xi) = L_{1j}(\xi) \tag{3.7}$$

where $L_{1j}(\xi)$ is the counterpart of $U_{1j}(\xi)$ in the lower half ξ -plane. Eliminate $B_j(\xi)$ from equation (3.5) and equation (3.7) and get

$$\frac{L_{1j}(\xi)}{U_{1j}(\xi)} = + \frac{K_{1j}}{2\pi i} \frac{1}{U_{1j}(\alpha_j)} \frac{S_{1j}\gamma_{j1}}{(\xi - \alpha_j)f'_j(\xi)} \tag{3.8}$$

To factor the right-hand side expression into the product of a U -function and an L -function, let

$$F_j(\xi) = \frac{2M_2^2}{[(1 + S_2^2)^2 - 4S_1S_2]} \frac{f'_j(\xi)}{(\xi - \xi_1)(\xi + \xi_2)} = F_{jL}(\xi)F_{jU}(\xi) \tag{3.9}$$

in which ξ_1 and $-\xi_2$ are the only zeros of $f'_j(\xi)$ and they are:

$$\xi_1 = \frac{S_2^2\lambda_{j2}}{C_R/C_2 + M_2} + M_j\lambda_{jj}, \quad \xi_2 = \frac{S_2^2\lambda_{j2}}{C_R/C_2 - M_2} - M_j\lambda_{jj} \tag{3.10}$$

with C_R being the Rayleigh surface velocity. For the solution of the roots of the function $f'_j(\xi)$, reference is made to Appendix A.

In view of equation (3.9), equation (3.8) assumes the form

$$\frac{L_{1j}(\xi)}{U_{1j}(\xi)} = + \frac{K'_{1j}}{U_{1j}(\alpha_j)} \left\{ \frac{[(1 - M_1)(\xi - M_j \lambda_{jj}) + S_1^2 \lambda_{j1}]^{\frac{1}{2}}}{(\xi + \xi_2) F_{jU}(\xi)} \right\} \left\{ \frac{[(1 + M_1)(\xi - M_j \lambda_{jj}) - S_1^2 \lambda_{j1}]^{\frac{1}{2}}}{(\xi - \alpha_j)(\xi - \xi_1) F_{jL}(\xi)} \right\} \quad (3.11)$$

where

$$K'_{1j} = \frac{1}{2\pi i} \frac{2M_2^2 K_{1j}}{[(1 + S_2^2)^2 - 4S_1 S_2]} \quad (3.12)$$

Hence, a solution is

$$U_{1j}(\xi) = \frac{(\xi + \xi_2) F_{jU}(\xi)}{[(1 - M_1)(\xi - M_j \lambda_{jj}) + S_1^2 \lambda_{j1}]^{\frac{1}{2}}}$$

$$L_{1j}(\xi) = + \frac{K'_{1j} [(1 - M_1)(\alpha_j - M_j \lambda_{jj}) + S_1^2 \lambda_{j1}]^{\frac{1}{2}} [(1 + M_1)(\xi - M_j \lambda_{jj}) - S_1^2 \lambda_{j1}]^{\frac{1}{2}}}{(\alpha_j + \xi_2) F_{jU}(\alpha_j) (\xi - \alpha_j)(\xi - \xi_1) F_{jL}(\xi)} \quad (3.13)$$

There remains the problem of the factorization of $F_j(\xi)$ into $F_{jL}(\xi)$ and $F_{jU}(\xi)$. In order to do so, define

$$G_j(s) = \log F_j(s), \quad \text{hence} \quad F_j(s) = \exp\{G_j(s)\} \quad (3.14)$$

If $G_j(s)$ can be decomposed into the sum

$$G_j(s) = G_{jU}(s) + G_{jL}(s)$$

then

$$F_{jU}(s) = \exp[G_{jU}(s)] \quad \text{and} \quad F_{jL}(s) = \exp[G_{jL}(s)].$$

Since $F(s)$ is analytic everywhere in the ξ -plane except at the cuts $(\beta_{j1} + \lambda_{j1}) \leq \text{Re}(s) \leq (\beta_{j2} + \lambda_{j2})$, $\text{Im}(s) = 0$ and $-(\lambda_{j2} - \beta_{j2}) \leq -\text{Re}(s) \leq -(\lambda_{j1} - \beta_{j1})$, $\text{Im}(s) = 0$, and $F_j(s) \rightarrow 1 + 0(1/s)$ as $|s| \rightarrow \infty$. Hence $G_j(s)$ is regular everywhere in cut s -plane and $G_j(s) \rightarrow 0(1/s)$ as $|s| \rightarrow \infty$. Therefore, by Cauchy's integral formula

$$G_j(s) = \frac{1}{2\pi i} \int_{C_U + C_L} \frac{G_j(z)}{z - s} dz \quad (3.15)$$

where the contours C_U and C_L in the z -plane are shown in Fig. 3. Equation (3.15) can further be written as

$$G_{jU,L}(s) = \frac{1}{2\pi i} \int_{C_U, C_L} \frac{G_j(z)}{z - s} dz$$

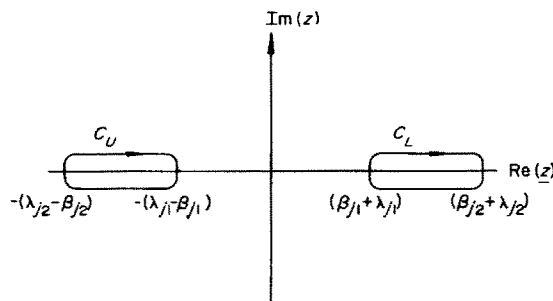


FIG. 3. Contour of integration in the z -plane.

and consequently

$$\begin{aligned}
 F_{jU}(s) &= \exp \left\{ \frac{1}{2\pi i} \int_{C_U} \frac{\log F_j(z)}{z-s} dz \right\} \\
 F_{jL}(s) &= \exp \left\{ \frac{1}{2\pi i} \int_{C_L} \frac{\log F_j(z)}{z-s} dz \right\}.
 \end{aligned}
 \tag{3.16}$$

Assume s doesn't lie on the cut for the moment and for a principal branch of the logarithmic function, equations (3.16) become

$$\begin{aligned}
 F_{jL}(s) &= \exp \left\{ \frac{1}{\pi} \int_{(\beta_{j1} + \lambda_{j1})}^{(\beta_{j2} + \lambda_{j2})} \Delta_j(z) \frac{dz}{z-s} \right\} \\
 F_{jU}(s) &= \exp \left\{ \frac{1}{\pi} \int_{(\beta_{j1} + \lambda_{j1})}^{(\beta_{j2} + \lambda_{j2})} \Delta_j(-z) \frac{dz}{z+s} \right\}
 \end{aligned}
 \tag{3.17}$$

in which

$$\Delta_j(z) = \tan^{-1} \frac{2S_1 S_2 \{ [(z - \beta_{j1})^2 - \lambda_{j1}^2] [\lambda_{j2}^2 - (z - \beta_{j2})^2] \}^{\frac{1}{2}} (z - M_j \lambda_{jj})^2}{\{ [(S_1^2/2C^2)\gamma_{j1}^2 - (1/2C^2 - 1)(z - M_j \lambda_{jj})^2] [z - M_j \lambda_{jj}]^2 + S_2^2 \gamma_{j2}^2 \}}.
 \tag{3.18}$$

When the point s approaches the branch cuts, the integrals defining F_{jU} and F_{jL} become singular. However, these integrals are obviously never singular simultaneously. Thus, F_{jU} and F_{jL} can be calculated by writing

$$F_{jU,L}(s) = \frac{2M_j^2}{[(1 + S_2^2)^2 - 4S_1 S_2]} \frac{f'_j(\xi)}{(\xi - \xi_1)(\xi + \xi_2) F_{jL,U}(\xi)}.
 \tag{3.19}$$

Equations (3.13) and (3.19) have thus completed the solution to the symmetric problem.

Case B. Skew-symmetric problem. Following the same procedure as in Case A, define

$$\begin{aligned}
 C_j(\xi) &= S_2 \gamma_{j2} D_j(\xi) = \{ [(1 + M_2)(\xi - M_j \lambda_{jj}) - S_2^2 \lambda_{j2}] \\
 &\quad \times [(1 - M_2)(\xi - M_j \lambda_{jj} + S_2^2 \lambda_{j2})] \}^{\frac{1}{2}} D_j(\xi)
 \end{aligned}
 \tag{3.20}$$

and then equations (2.48) become

$$\begin{aligned}
 \frac{1}{2\pi} \int_{-\infty}^{\infty} S_2 \gamma_{j2} D_j(\xi) \exp(-i\xi x) d\xi &= 0, \quad x > 0 \\
 \frac{1}{2\pi} \int_{-\infty}^{\infty} f'_j(\xi) D_j(\xi) \exp(-i\xi x) d\xi &= -Q_j \exp(-i\lambda_{jj} x \cos \theta_j), \quad x < 0.
 \end{aligned}
 \tag{3.21}$$

Without going into details, this set of dual integral equations can be solved by exactly the same procedure as in Case A and the result is

$$\begin{aligned}
 U_{2j}(\xi) &= \frac{(\xi + \xi_2) F_{jL}(\xi)}{[(1 - M_2)(\xi - M_j \lambda_{jj}) + S_2^2 \lambda_{j2}]^{\frac{1}{2}}} \\
 S_2 \gamma_{j2} D_j(\xi) = L_{2j}(\xi) &= + \frac{K'_{2j} [(1 - M_2)(\alpha_j - M_j \lambda_{jj}) + S_2^2 \lambda_{j2}]^{\frac{1}{2}}}{(\alpha_j + \xi_2) F_{jU}(\alpha_j)} \\
 &\quad \times \frac{[(1 + M_2)(\xi - M_j \lambda_{jj}) - S_2^2 \lambda_{j2}]^{\frac{1}{2}}}{(\xi - \alpha_j)(\xi - \xi_1) F_{jL}(\xi)}
 \end{aligned}
 \tag{3.22}$$

in which

$$k'_{2j} = \frac{1}{2\pi i} \frac{2M_2^2}{[(1+S_2^2)^2 - 4S_1S_2]} (-2\pi Q_j) \tag{3.23}$$

and the functions U_{2j} and L_{2j} have the same behavior as U_{1j} and L_{1j} , respectively.

Singular stresses around the moving crack tip

The analytical purpose of fracture mechanics is to study the state of stress immediately around the crack tip. This provides the connection between the stresses which control crack propagation and the applied loads. In the ensuing discussion, the dynamic stress fields for Case A and Case B will be examined separately.

Case A. Symmetric problem. Combining equations (3.2), (3.7) and (3.13) yields

$$A_j(\xi) = + \frac{k'_{1j}[(1 - M_1)(\alpha_j - M_j\lambda_{jj}) + S_1^2\lambda_{j1}]^{\frac{1}{2}}}{(\alpha_j + \xi_2)F_{jU}(\alpha_j)} \frac{[(1 + M_1)(\xi - M_j\lambda_{jj}) - S_1^2\lambda_{j1}]^{\frac{1}{2}}}{(\xi - \alpha_j)(\xi - \xi_1)F_{jL}(\xi)} \tag{3.24}$$

The singular behavior of the stress components for the scattered waves at the crack tip is due to the divergence of the improper integrals around $x = y = 0$ in equations (2.20). This divergence is contributed by the behavior of the corresponding integrands as $\xi \rightarrow \infty$. Making use of equations (2.28) and (3.24), asymptotic expansions of the integrands appearing in equations (2.20) for large values of ξ lead to

$$\begin{aligned} \sigma_x^{(s)} &= A \int_0^\infty \{ (1 + S_1^2)(1 - S_2^2 + 2S_1^2)[\xi^{-\frac{1}{2}} \exp(-S_1\xi y - i\xi x) \\ &\quad - i\xi^{-\frac{1}{2}} \exp(-S_1\xi y + i\xi x)] - 4S_1S_2[\xi^{-\frac{1}{2}} \exp(-S_2\xi y - i\xi x) \\ &\quad - i\xi^{-\frac{1}{2}} \exp(-S_2\xi y + i\xi x)] \} d\xi, \\ \sigma_y^{(s)} &= A \int_0^\infty \{ -(1 + S_2^2)^2[\xi^{-\frac{1}{2}} \exp(-S_1\xi y - i\xi x) - i\xi^{-\frac{1}{2}} \exp(-S_1\xi y + i\xi x)] \\ &\quad + 4S_1S_2[\xi^{-\frac{1}{2}} \exp(-S_2\xi y - i\xi x) - i\xi^{-\frac{1}{2}} \exp(-S_2\xi y + i\xi x)] \} d\xi, \\ \sigma_{xy}^{(s)} &= A \cdot 2S_1(1 + S_2^2) \int_0^\infty (-1) \{ [\xi^{-\frac{1}{2}} \exp(-S_1\xi y - i\xi x) \\ &\quad - i\xi^{-\frac{1}{2}} \exp(-S_1\xi y + i\xi x)] - [\xi^{-\frac{1}{2}} \exp(-S_2\xi y - i\xi x) \\ &\quad + i\xi^{-\frac{1}{2}} \exp(-S_2\xi y + i\xi x)] \} d\xi \end{aligned} \tag{3.25}$$

where

$$A = - \frac{\mu k'_{1j}[(\alpha_j - M_j\lambda_{jj}) + (1 + M_1)\lambda_{j1}]^{\frac{1}{2}}}{2\pi M_2^2(\alpha_j + \xi_2)F_{jU}(\alpha_j)} \tag{3.26}$$

Since the stress field of the incident waves are non-singular, the unbounded contributions to the total stress field near the origin are precisely equal to those of the scattered

waves. Carrying out the integration and rearranging the constant terms yield the following :

$$\begin{aligned}\sigma_x &= \frac{k_1}{[4S_1S_2 - (1 + S_2^2)^2]} \frac{1}{(2r)^{\frac{1}{2}}} \{(1 + S_2^2)(1 - S_2^2 + 2S_1^2)f(S_1) - 4S_1S_2f(S_2)\} + 0(1), \\ \sigma_y &= \frac{k_1}{[4S_1S_2 - (1 + S_2^2)^2]} \frac{1}{(2r)^{\frac{1}{2}}} \{4S_1S_2f(S_2) - (1 + S_2^2)^2f(S_1)\} + 0(1), \\ \sigma_{xy} &= \frac{k_1}{[4S_1S_2 - (1 + S_2^2)^2]} \frac{1}{(2r)^{\frac{1}{2}}} 2S_1(1 + S_2^2) \{g(S_1) - g(S_2)\} + 0(1)\end{aligned}\quad (3.27)$$

where

$$\begin{aligned}f^2(S_j) + g^2(S_j) &= \sec \phi \cdot (1 + S_j^2 \tan^2 \phi)^{-\frac{1}{2}} \\ f^2(S_j) - g^2(S_j) &= \sec \phi \cdot (1 + S_j^2 \tan^2 \phi)^{-1}\end{aligned}\quad (3.28)$$

and

$$r = (x^2 + y^2)^{\frac{1}{2}}; \quad \phi = \tan^{-1} \left(\frac{y}{x} \right).\quad (3.29)$$

The parameter k_1 in equations (3.27) is defined by

$$k_1 = \left(\frac{2}{\pi} \right)^{\frac{1}{2}} \frac{[(\alpha_j - M_j \lambda_{jj}) + (1 + M_1) \lambda_{j1}]^{\frac{1}{2}}}{(\alpha_j + \xi_2) F_{j\nu}(\alpha_j)} \sigma_j \exp \left(\frac{\pi i}{4} \right)\quad (3.30)$$

in which

$$\sigma_j = +2\mu P_j.\quad (3.31)$$

Case B. Skew-symmetric problem. Following the same procedure as in Case A, the singular portion of the stress field can be found as

$$\begin{aligned}\sigma_x &= \frac{k_2}{[4S_1S_2 - (1 + S_2^2)^2]} \frac{1}{(2r)^{\frac{1}{2}}} 2S_2 \{(1 + S_2^2)g(S_2) - (1 - S_2^2 + 2S_1^2)g(S_1)\}, \\ \sigma_y &= \frac{k_2}{[4S_1S_2 - (1 + S_2^2)^2]} \frac{1}{(2r)^{\frac{1}{2}}} 2S_2(1 + S_2^2) \{g(S_1) - g(S_2)\}, \\ \sigma_{xy} &= \frac{k_2}{[4S_1S_2 - (1 + S_2^2)^2]} \frac{1}{(2r)^{\frac{1}{2}}} \{4S_1S_2f(S_1) - (1 + S_2^2)^2f(S_2)\}\end{aligned}\quad (3.32)$$

in which

$$k_2 = \left(\frac{2}{\pi} \right)^{\frac{1}{2}} \frac{[(\alpha_j - M_j \lambda_{jj}) + (1 + M_2) \lambda_{j2}]^{\frac{1}{2}}}{(\alpha_j + \xi_2) F_{j\nu}(\alpha_j)} \tau_j \exp \left(\frac{\pi i}{4} \right)\quad (3.33)$$

and

$$\tau_j = +2\mu Q_j.\quad (3.34)$$

In view of equation (3.23) the actual stress components σ_x , σ_y and σ_{xy} can be found from σ_x , σ_y and σ_{xy} by modifying the factors k_1 and k_2 . Let K_1 and K_2 denote these modified factors and they are taken to be the dynamic stress-intensity factor:

$$\begin{aligned}
 K_1 &= k_1 \exp(iM_j \lambda_{jj} x - i\omega_j t) = \left(\frac{2}{\pi}\right)^{\frac{1}{2}} \\
 &\times \frac{[(\alpha_j - M_j \lambda_{jj}) + (1 + M_1) \lambda_{j1}]^{\frac{1}{2}}}{(\alpha_j + \xi_2) F_{jU}(\alpha_j)} \sigma_j \exp\left\{i\left[M_j \lambda_{jj} x + \frac{\pi}{4} - \omega_j t\right]\right\}, \quad (3.35) \\
 K_2 &= k_2 \exp(iM_j \lambda_{jj} x - i\omega_j t) = \left(\frac{2}{\pi}\right)^{\frac{1}{2}} \\
 &\times \frac{[(\alpha_j - M_j \lambda_{jj}) + (1 + M_2) \lambda_{j2}]^{\frac{1}{2}}}{(\alpha_j + \xi_2) F_{jU}(\alpha_j)} \tau_j \exp\left\{i\left[M_j \lambda_{jj} x + \frac{\pi}{4} - \omega_j t\right]\right\}.
 \end{aligned}$$

The inverse square root of r stress singularity is found to be identical to that of stationary crack problem [33]. However, the angular variation of the stresses in ϕ around the crack tip is distorted by the speed of crack propagation. In addition, the intensity factors K_1 and K_2 differ significantly from the static solutions since they fluctuate in time and are proportional to the circular frequency, amplitude of input wave, angle of incidence and speed of crack propagation.

As $v \rightarrow 0$, the stresses become

$$\begin{aligned}
 \sigma_x &= \frac{K_1^*}{(2r)^{\frac{1}{2}}} \cos \frac{\phi}{2} \left[1 - \sin \frac{\phi}{2} \sin \frac{3\phi}{2}\right] + 0(1) \\
 \sigma_y &= \frac{K_1^*}{(2r)^{\frac{1}{2}}} \cos \frac{\phi}{2} \left[1 + \sin \frac{\phi}{2} \sin \frac{3\phi}{2}\right] + 0(1) \\
 \sigma_{xy} &= \frac{K_1^*}{(2r)^{\frac{1}{2}}} \cos \frac{\phi}{2} \sin \frac{\phi}{2} \cos \frac{3\phi}{2} + 0(1)
 \end{aligned} \quad (3.36)$$

for Case A and

$$\begin{aligned}
 \sigma_x &= -\frac{K_2^*}{(2r)^{\frac{1}{2}}} \sin \frac{\phi}{2} \left[2 + \cos \frac{\phi}{2} \cos \frac{3\phi}{2}\right] + 0(1) \\
 \sigma_y &= \frac{K_2^*}{(2r)^{\frac{1}{2}}} \sin \frac{\phi}{2} \cos \frac{\phi}{2} \cos \frac{3\phi}{2} + 0(1) \\
 \sigma_{xy} &= \frac{K_2^*}{(2r)^{\frac{1}{2}}} \cos \frac{\phi}{2} \left[1 - \sin \frac{\phi}{2} \sin \frac{3\phi}{2}\right] + 0(1)
 \end{aligned} \quad (3.37)$$

for Case B; where

$$\begin{aligned}
 K_1^* &= \left(\frac{2}{\pi}\right)^{\frac{1}{2}} \frac{[\Lambda_j \cos \Theta_j + \Lambda_1]^{\frac{1}{2}} \sigma_j^*}{[\Lambda_j \cos \Theta_j + \Lambda_1 (C_1/C_R)] F_{jU}^*(\Lambda_j \cos \Theta_j)} \exp\left(\frac{\pi}{4} i - i\Omega t\right) \\
 K_2^* &= \left(\frac{2}{\pi}\right)^{\frac{1}{2}} \frac{[\Lambda_j \cos \Theta_j + \Lambda_2]^{\frac{1}{2}} \tau_j^*}{[\Lambda_j \cos \Theta_j + \Lambda_2 (C_2/C_R)] F_{jU}^*(\Lambda_j \cos \Theta_j)} \exp\left(\frac{\pi}{4} i - i\Omega t\right) \\
 F_{jU}^*(s) &= \exp\left\{\frac{1}{\pi} \int_{\Lambda_1}^{\Lambda_2} \tan^{-1} \frac{4z^2 [(z^2 - \Lambda_1^2)(\Lambda_2^2 - z^2)]^{\frac{1}{2}} dz}{(2z^2 - \Lambda_2^2)^2} \frac{dz}{z+s}\right\}.
 \end{aligned} \quad (3.38)$$

$$(3.39)$$

In equations (3.38), σ_j^* and τ_j^* are defined as the value of σ_j and τ_j as $v \rightarrow 0$, respectively. Thus, K_1^* and K_2^* denote the strength of the singularities near the crack tip for a stationary crack subject to the action of input stress waves. Adopting the criterion in the theory of brittle fracture [33], K_1^* and K_2^* may be regarded as the dynamic stress-intensity factors the critical value of which are functions of material property and can be measured experimentally to determine the point of incipient fracture.

The influence of the crack propagating speed upon the K_1 factor can best be illustrated by a plot of K_1/K_1^* vs the velocity ratio v/c_1 . For a P-wave incident on the crack in the state of generalized plane stress, Fig. 4 shows the behavior of K_1/K_1^* against v/c_1 for various

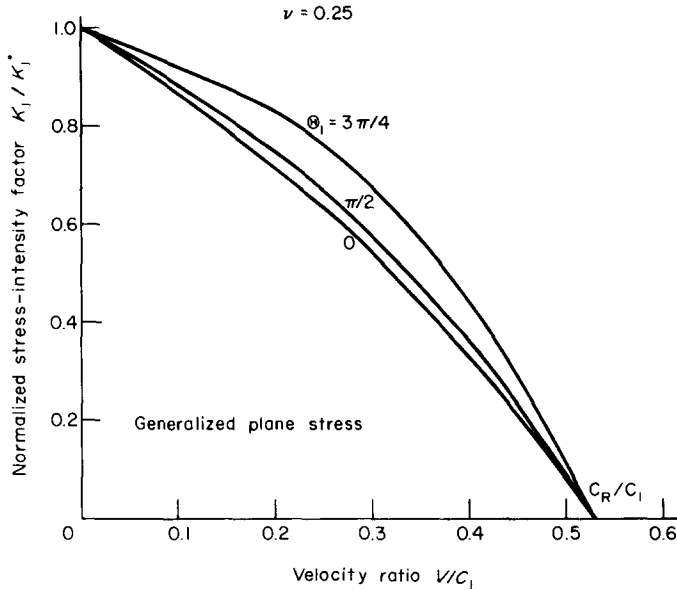


FIG. 4. Variation of K_1/K_1^* vs V/C_1 for different Θ_1 —semi-infinite crack and P-wave incidence.

angles of incidence. The value of K_1/K_1^* decreases as v/c_1 increases and falls to zero as Rayleigh wave speed is reached. In Fig. 5 the variations of K_1/K_1^* vs v/c_1 for a P-wave incident normally on the crack with different Poisson's ratios are presented. The value of K_1 increases as the compressibility of the material is increased and all the curves drop to zero as v reaches the Rayleigh wave velocity, which is the root of the denominator $[4S_1S_2 - (1 + S_2^2)^2]$. This same behavior has also been found by [34], among others, for a propagating crack subject to uniform tension at infinity.

Let the crack be excited by SV-waves and consider a state of generalized plane stress. As is evident from Fig. 6, the variation of K_2/K_2^* with V/C_2 for various angles of incidence follows the same trend as that of Fig. 4. In Fig. 7, K_2 decreases when the Poisson's ratio is decreased, as it should for the skew-symmetric problem.

Also, the stress-intensity factor can be influenced by the input wave amplitude. The K -factors will increase as the wave amplitude is increased.

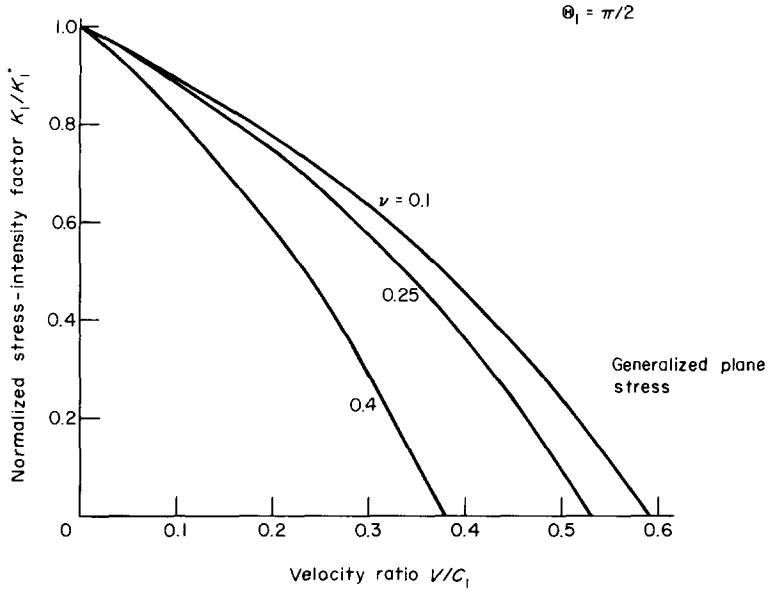


FIG. 5. Variation of K_1/K_1^* vs V/C_1 for different ν —semi-infinite crack and P -wave incidence.

Crack opening displacement

If a medium containing a crack is subjected to the action of stress waves, the interference which the crack surface experiences may alternate in sign depending upon whether the incident field is tensile or compressive. This will cause the opposing crack surfaces to come into contact and thus violating the assumption of a traction-free crack. Hence, an

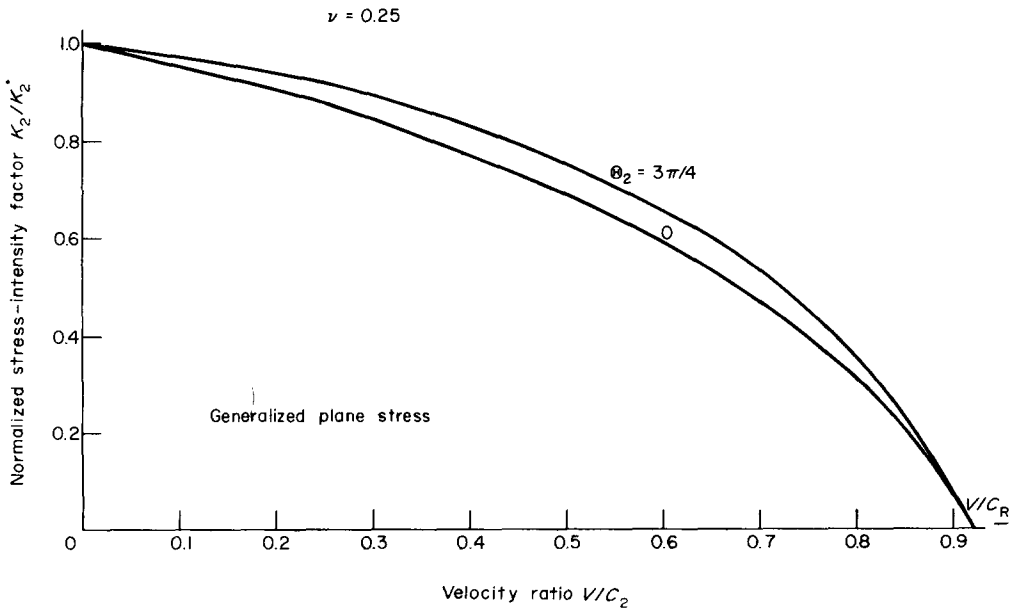


FIG. 6. Variation of K_2/K_2^* vs V/C_2 for different θ_2 —semi-infinite crack and SV -wave incidence.

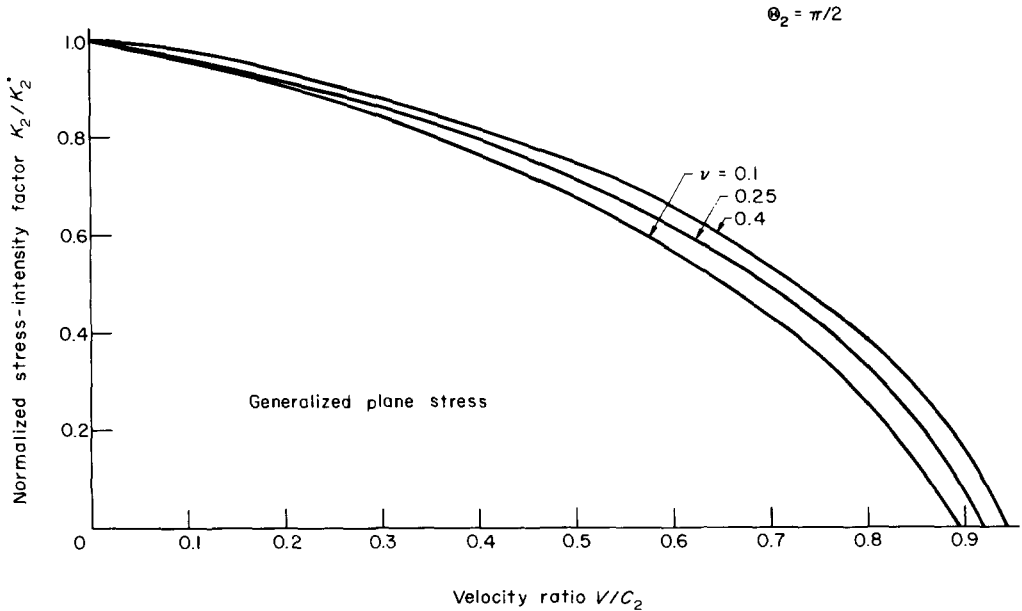


FIG. 7. Variation of K_2/K_2^* vs V/V_2 for different ν —semi-infinite crack and SV -wave incidence.

additional tensile stress field must be added to keep the crack surface separated. The displacement solution of the original problem provides an estimation of the requisite tensile field.

For the symmetric case, the quantity of interest is the normal displacement

$$v_y(x, 0) = \frac{ik'_{1j}[(1 - M_1)(\alpha_j - M_j\lambda_{jj}) + S_1^2\lambda_{j1}]^{\frac{1}{2}}}{(\alpha_j + \xi_2)(\alpha_j - \xi_1)F_{jV}(\alpha_j)F_{jL}(\alpha_j)} \{ [(1 + M_1)(\alpha_j - M_j\lambda_{jj}) - S_1^2\lambda_{j1}]^{\frac{1}{2}} \exp(-i\alpha_j x) - [(1 + M_1)(\xi_1 - M_j\lambda_{jj}) - S_1^2\lambda_{j1}]^{\frac{1}{2}} \frac{F_{jL}(\alpha_j)}{F_{jL}(\xi_1)} \exp(-i\xi_1 x) \}, \quad x < 0. \tag{3.40}$$

The numerical calculation of equation (3.40) will be carried out for the case of normal incidence, $\Theta_1 = \pi/2$. Figures 9 and 10 display the amplitude of $V_y(x, 0)$ given by equation (3.40) for several values of M_1 . At low frequencies and close to the crack tip, Fig. 8 shows that the crack opens like an ellipse in the dynamic case, just as in the static case. But at high frequencies and away from the crack tip, the multiple interferences on the crack surface introduce oscillations in these curves as shown in Fig. 9. In order to keep the crack surfaces from getting into contact, the opening displacement shown by the curves in Fig. 9 should at least be doubled so that during compression cycles sufficient clearance is provided. As expected, the maximum value of $|\mu v_y(x, 0)\Lambda_1/\sigma_1| \approx 1.06$ occurs at $M_1 = 0$, the velocity ratio at which the dimensionless stress-intensity factor is also a maximum. Generally speaking, at higher crack velocities the peak values of the crack opening displacements tend to decrease and occur further away from the crack tip.

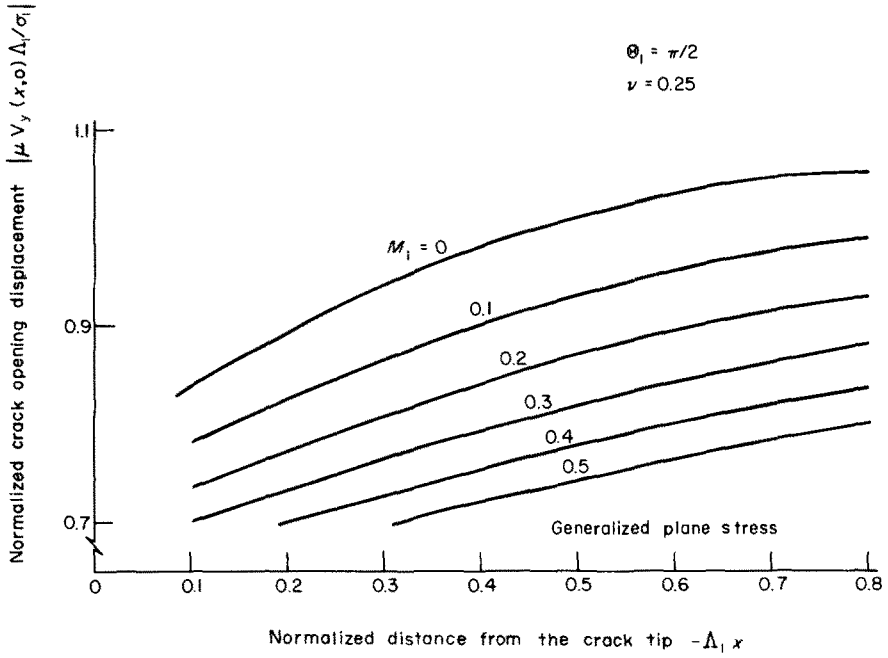


FIG. 8. Variation of crack opening displacement close to the crack-tip—semi-infinite crack.

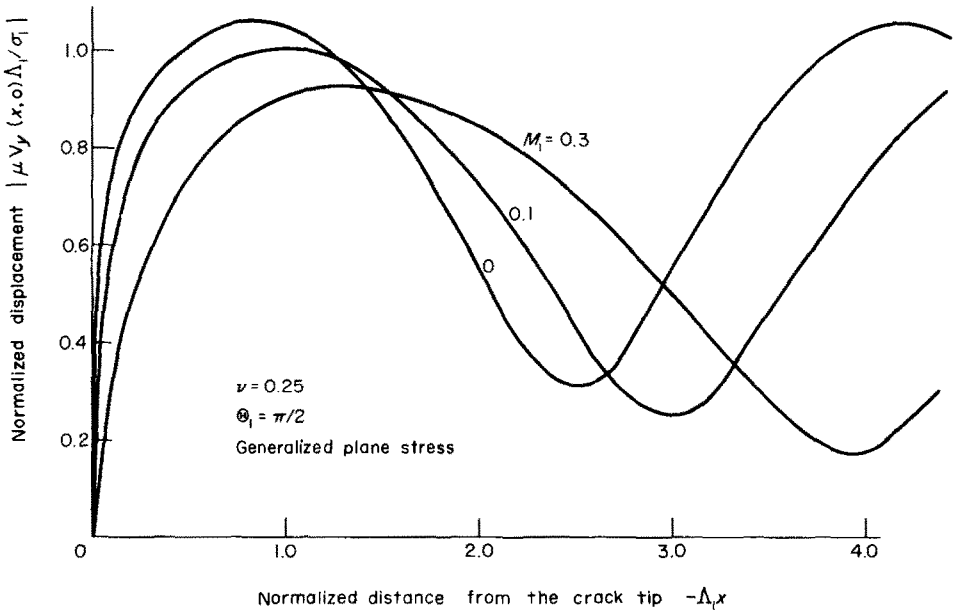


FIG. 9. Variation of crack opening displacement vs distance from the crack-tip—semi-infinite crack.

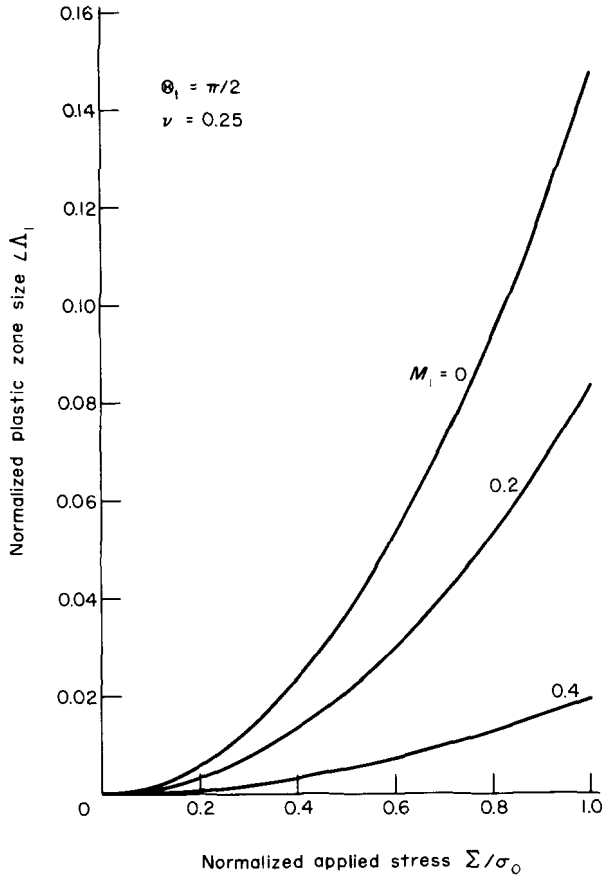


FIG. 10. $L\Delta_1$ vs Σ_1/σ_0 for different M_1 —normal incidence and $\nu = 0.25$.

4. DUCTILE CRACK PROPAGATION

Construction of Dugdale's model

Consider the diffraction problem of a semi-infinite propagating crack travelling at constant velocity v in an infinite medium. Both stationary coordinates X, Y and moving coordinates x, y are introduced. The solution will be obtained by employing the Dugdale's hypothesis and the assumption that application of a load always produces a yield zone in the plane of the crack.

Applying the principle of superposition, two sub-problems are created the sum of which yields the solution to the original problem. These sub-problems are:

Sub-problem A. A semi-infinite crack occupying the space $x < 0, y = 0$ in the moving coordinate system is subjected to the action of impinging stress waves from infinity. The surfaces of the crack are assumed to be traction-free and the stress at infinity can be derived from the incident wave potentials. This is exactly the problem solved in Section 3. For

symmetrical loading the near field stresses can be expressed as

$$\begin{aligned} \sigma_x &= \frac{K_1}{[4S_1S_2 - (1 + S_2^2)^2]} \frac{1}{(2r)^{\frac{1}{2}}} \{(1 + S_2^2)(1 - S_2^2 + 2S_1^2)f(S_1) - 4S_1S_2f(S_2)\} + 0(1) \\ \sigma_y &= \frac{K_1}{[4S_1S_2 - (1 + S_2^2)^2]} \frac{1}{(2r)^{\frac{1}{2}}} \{4S_1S_2f(S_2) - (1 + S_2^2)^2f(S_1)\} + 0(1) \\ \sigma_{xy} &= \frac{K_1}{[4S_1S_2 - (1 + S_2^2)^2]} \frac{1}{(2r)^{\frac{1}{2}}} 2S_1(1 + S_2^2)\{g(S_1) - g(S_2)\} + 0(1) \end{aligned} \tag{4.1}$$

where the stress-intensity factor K_1 is defined in equation (3.35) and the functions f and g have been given in equations (3.28).

Sub-problem B. In this case, a semi-infinite crack on $y = 0, x < 0$ extending at velocity v , is acted upon by running normal stresses $-\sigma_0$ on the faces over a length l behind the tip. At infinity it is assumed to be stress-free. This problem has been treated by several authors [19], [36], using the theory of complex variables. Thus, the stresses around the crack-tip can be written as [36]

$$\begin{aligned} \sigma_x &= \frac{K_{1p}}{[4S_1S_2 - (1 + S_2^2)^2]} \frac{1}{(2r)^{\frac{1}{2}}} \{(1 + S_2^2)(1 - S_2^2 + 2S_1^2)f(S_1) - 4S_1S_2f(S_2)\} + 0(1) \\ \sigma_y &= \frac{K_{1p}}{[4S_1S_2 - (1 + S_2^2)^2]} \frac{1}{(2r)^{\frac{1}{2}}} \{4S_1S_2f(S_2) - (1 + S_2^2)^2f(S_1)\} + 0(1) \\ \sigma_{xy} &= \frac{K_{1p}}{[4S_1S_2 - (1 + S_2^2)^2]} \frac{1}{(2r)^{\frac{1}{2}}} 2S_1(1 + S_2^2)\{g(S_1) - g(S_2)\} + 0(1) \end{aligned} \tag{4.2}$$

in which the plastic intensity factor K_{1p} is defined as

$$K_{1p} = -\frac{2}{\pi} \sigma_0 (2l)^{\frac{1}{2}}. \tag{4.3}$$

Consequently, the superposition of sub-problems A and B gives rise to the diffraction problem of a running Dugdale crack.

Determination of the plastic zone size

Since the presence of the yield zone should remove the singularity at the crack tip, the condition $K_1 + K_{1p} = 0$ must be fulfilled. Making use of equation (3.38) and equation (4.3) the finiteness condition yields the following result:

$$\left(\frac{2}{\pi}\right)^{\frac{1}{2}} \frac{[(\alpha_j - M_j \lambda_{j1} \varepsilon + (1 + M_1) \lambda_{j1})^{\frac{1}{2}} \sigma_j \exp\left\{i\left(M_j \lambda_{jj} x + \frac{\pi}{4} - \omega_j t\right)\right\}]}{(\alpha_j + \xi_2) F_{jU}(\alpha_j)} = \frac{2}{\pi} \sigma_0 (2l)^{\frac{1}{2}}.$$

The above expression can be simplified to

$$\frac{\sum_j}{\sigma_0} = \frac{2(l)^{\frac{1}{2}} (\alpha_j + \xi_2) F_{jU}(\alpha_j)}{(\pi)^{\frac{1}{2}} [(\alpha_j - M_j \lambda_{jj}) + (1 + M_1) \lambda_{j1}]^{\frac{1}{2}}} \tag{4.4}$$

where $\sum_j = \sigma_j \exp\{i[M_j \lambda_{jj} + \pi/4 - \omega_j t]\}$ represent the external load. Equation (4.4) completely determines the length of the plastic zone.

Numerical results have been obtained for the dimensionless quantity $l\Lambda_1$ as a function of Σ_1/σ_0 , Θ_1 and M_1 under the influence of incident P-waves. Figure 10 shows the variations of normalized plastic zone length $l\Lambda_1$ vs the ratio Σ_1/σ_0 for several values of M_1 under normal incident stress waves. The Poisson's ratio of the material is taken to be 0.25. These curves exhibit that the length of the plastic zone decreases as the velocity of the crack increases. This is in agreement with the observation made by Atkinson [28] in solving the problem of a symmetrical growing crack employing the Dugdale's hypothesis. The plastic zone length reduces to zero as the velocity approaches the Rayleigh wave velocity which implies that no yielding takes place when the crack is running at Rayleigh wave velocity. Finally, for completeness the normalized plastic zone length is plotted in Fig. 11 against the velocity ratio M_1 for various values of the ratio Σ_1/σ_0 . The angle of incidence is again taken as $\pi/2$ and the Poisson's ratio of the material is 0.25. The curves show that the plastic extension is longer at smaller yield stress, a phenomenon which is in agreement with observation.

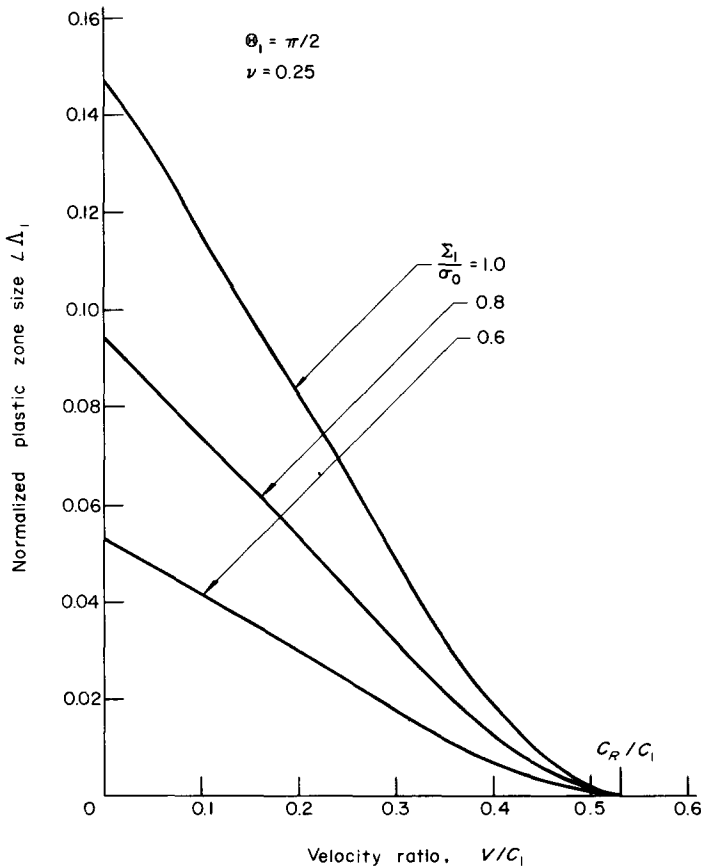


FIG. 11. $l\Lambda_1$ vs M_1 for different Σ_1/σ_0 —normal incidence and $\nu = 0.25$.

Acknowledgement—This work is part of the research program supported by the U.S. Navy through the Office of Naval Research under Grant N0014-68-A-0514.

REFERENCES

- [1] D. ANG and L. KNOPOFF, Diffraction of scalar elastic waves by a finite crack. *Proc. Nat. Acad. Sci.* **51**, 593 (1964).
- [2] D. ANG and L. KNOPOFF, Diffraction of vector elastic waves by a finite crack. *Proc. Nat. Acad. Sci.* **51**, 1075 (1964).
- [3] J. LOEBER and G. SIH, Diffraction of anti-plane shear waves by a finite crack. *J. acoust Soc. Am.* **44**, 90 (1968).
- [4] G. SIH and J. LOEBER, Torsional vibration of an elastic solid containing a penny-shaped crack. *J. acoust Soc. Am.* **44**, 1237 (1968).
- [5] G. SIH and J. LOEBER, Normal compression and radial shear waves scattering at a penny-shaped crack in an elastic solid. *J. acoust Soc. Am.* **46**, 711 (1969).
- [6] G. SIH and J. LOEBER, Wave propagation in an elastic solid with a line of discontinuity or finite crack, *Quart. appl. Math.* **27**, 193 (1969).
- [7] B. BAKER, Dynamic stresses created by a moving crack. *J. appl. Mech.* **29**, 449 (1962).
- [8] R. RAVERA, On Some Elastodynamic Problems with Geometrical Singularities, Ph.D. Dissertation, Lehigh University, (1967).
- [9] G. EMBLEY, Impact Loadings of Cracks in Elastic Bodies, Ph.D. Dissertation, Lehigh University, (1970).
- [10] S. THAU and T. LU, Diffraction of transient horizontal shear waves by a finite crack and a finite rigid ribbon. *Int. J. of Eng. Sci.* **8**, 857 (1970).
- [11] S. THAU and T. LU, Transient stress intensity factors for a finite crack in an elastic solid caused by a dilatational wave. *Int. J. Solids Struct.* **7**, 731 (1971).
- [12] J. EVVARD, Distribution of Waves Drag and Lift in the Vicinity of Wing Tips at Supersonic Speeds. National Advisory Committee for Aeronautics, Technical Note No. 1382 (1947).
- [13] B. KOSTROV, Unsteady crack propagation for longitudinal shear cracks. *J. appl. Math. Mech. (PMM)* **30**, 1042 (1966).
- [14] J. ACHENBACH, Crack propagation generated by a horizontally polarized shear wave. *J. Mech. Phys. Solids* **18**, 245 (1970).
- [15] J. ACHENBACH, Extension of a crack by a shear wave. *Z. Angew. Math. Phys.* **21**, 887 (1970).
- [16] J. ACHENBACH, Brittle and ductile extension of a finite crack by a horizontally polarized shear wave, *Int. J. Eng. Sci.* **8**, 947 (1970).
- [17] J. ACHENBACH and R. NUISMER, Fracture generated by a dilatational wave. *Int. J. Fracture Mech.* **7**, 77 (1971).
- [18] E. YOFFE, The moving Griffith crack. *Phil. Mag.* **42**, Series 7, 739 (1951).
- [19] J. CRAGGS, On the propagation of a crack in an elastic brittle material. *J. Mech. Phys. Solids* **8**, 66 (1960).
- [20] K. BROBERG, The propagation of a brittle crack. *Arkiv för Fysik.* **18**, 159 (1960).
- [21] J. CRAGGS, Fracture criteria for use in continuum mechanics. *Fracture of Solids*, pp. 51–63. John Wiley (1963).
- [22] C. ATKINSON, On axially symmetric boundary value problems in classical elasticity. *Int. J. Eng. Sci.* **6**, 27 (1968).
- [23] B. KOSTROV, The axisymmetric problem of propagation of a tensile crack. *J. appl. Math. Mech. (PMM)* **28**, 644 (1964).
- [24] A. JAHANSHAH, A diffraction problem and crack propagation. *J. appl. Mech.* **34**, 100 (1967).
- [25] G. SIH and J. LOEBER, Interaction of horizontal shear waves with a running crack. *J. appl. Mech.* **37**, 324 (1970).
- [26] D. DUGDALE, Yielding of Steel Sheets Containing Slits. *J. Mech. Phys. Solids* **8**, 100 (1960).
- [27] J. GOODIER and F. FIELDS, Plastic energy dissipation in crack propagation. *Fracture of Solids*, pp. 103–118, John Wiley (1963).
- [28] C. ATKINSON, A simple model of relaxed expanding crack. *Arkiv för Fysik.* **35**, 459 (1967).
- [29] M. KANNINEN, An estimate of the limiting speed of a propagating ductile crack. *J. Mech. Phys. Solids* **16**, 215 (1968).
- [30] G. EMBLEY and G. SIH, Plastic Flow Around an Expanding Crack. Technical Report AF-TR-71-2, Inst. of Fracture and Solid Mechanics, Lehigh University, (1971).
- [31] M. KANNINEN, A. MUKHERJEE, A. ROSENFELD and G. HAHN, The speed of ductile-crack propagation and the dynamics of flow in metals. *Mechanical Behavior of Materials Under Dynamic Loads*, pp. 96–133. Springer (1968).
- [32] B. NOBLE, *Method Based on the Wiener-Hopf Technique for the Solution of Partial Differential Equations*. Pergamon Press (1958).
- [33] G. SIH and H. LIEBOWITZ, Mathematical Theories of Brittle Fracture. *Fracture*, Vol. 2. Academic Press (1968).
- [34] B. COTTERELL, On the nature of moving cracks. *J. appl. Mech.* **31**, 12 (1964).

- [35] G. Sih, Dynamic Aspects of Crack Propagation. Technical Report No. 1, Department of Mechanical Engineering and Mechanics, Lehigh University (1969).
 [36] G. Sih, Some elastodynamic problems of cracks. *Int. J. Fracture Mech.* **5**, 51 (1968).

APPENDIX A

Solution for the roots of the function $f'_j(\xi)$.

From equations (2.30) and (3.4) $f'_j(\xi)$ can be written as

$$f'_j(\xi) = \frac{\{(S_1^2/2C^2)\gamma_{j1}^2 - [(1/2C^2) - 1]\sigma^2\}[\sigma^2 + S_2^2\gamma_{j2}^2] - 2S_1S_2\gamma_{j1}\gamma_{j2}\sigma^2}{[\sigma^2 - S_2^2\gamma_{j2}^2]} \quad (\text{A.1})$$

where

$$\sigma = \xi - M_j\lambda_{jj}. \quad (\text{A.2})$$

Making use of equations (2.19) and (A.2), equation (2.21) renders

$$\gamma_{jk}^2 = \sigma^2 + 2M_k\lambda_{jk}\sigma - S_k^2\lambda_{jk}^2. \quad (\text{A.3})$$

Upon substitution of equation (A.3) into equation (A.1) it becomes

$$f'_j(\xi) = \frac{(2\sigma^2 - \alpha^2)^2 - 4\sigma^2[(\sigma^2 - C^2\alpha^2)(\sigma^2 - \alpha^2)]^{\frac{1}{2}}}{2\alpha^2} \quad (\text{A.4})$$

in which

$$\alpha^2 = \sigma^2 - S_2^2\gamma_{j2}^2 = (M_2\sigma - S_2^2\lambda_{j2})^2. \quad (\text{A.5})$$

The numerator in equation (A.4) can readily be identified as the Rayleigh's function and the roots are:

$$\alpha^2 = \frac{\sigma^2 C_R^2}{C_2^2}, \quad \alpha^2 = 0 \quad (\text{A.6})$$

where C_R denotes the Rayleigh surface wave velocity. Since $\alpha^2 = 0$ are also roots for the denominator of $f'_j(\xi)$, they cannot be roots for the function $f'_j(\xi)$.

Consequently, the roots of $f'_j(\xi)$ are:

$$\alpha^2 = \frac{\sigma^2 C_R^2}{C_2^2} \quad (\text{A.7})$$

or they can be put in the form

$$(M_2 \mp C_R/C_2)(\xi - M_j\lambda_{jj}) = S_2^2\lambda_{j2}. \quad (\text{A.8})$$

(Received 31 July 1972)

Абстракт—В работе исследуется стационарная дифракция волн напряжения посредством полубесконечной, движущейся трещины. В месте с принципом суперпозиции, получается строгое решение путем применения метода, основанного на способе Винера-Хопфа. Так как для статического случая, динамические напряжения обладают хорошо знакомой особой точкой обратно пропорционально квадратному корню в конце трещины. Тем не менее, факторы интенсивности напряжений зависят от длины ударяющей волны, угла падения, коэффициента Пуассона упругого твердого тела и скорости распространения трещины. Фактор интенсивности напряжений является полезным параметром для исследования упругодинамических задач трещины, так как он может быть соединенным со скоростью, при которой упругая и кинетическая энергии освобождаются трещиной. Исследуется пластическое разрушение, приспособляя гипотезу Даггрейла. Определяется длина пластической зоны. Показывается графически влияние скорости распространения трещины.